Supplemental Material

LIST OF TABLES

Table S1. The SW modeling experiments for isolating the contribution from different tropical ocean basins in forming the springtime North Pacific ENSO teleconnection bias during La Niña events. Basic state is the FM climatology of winds and temperature during 1958 to 2010. Diabatic heating anomalies is composited during FM of the La Niña years. 2

Table S1. The SW modeling experiments for isolating the contribution from different tropical ocean basins in forming the springtime North Pacific ENSO teleconnection bias during La Niña events. Basic state is the FM climatology of winds and temperature during 1958 to 2010. Diabatic heating anomalies is composited during FM of the La Niña years.

Experiment Name	Heating
LN_trop	TOGA−JRA (15°S-15°N)
LN_IO	TOGA−JRA (15°S-15°N, 40°E-110°E)
LN_WP	TOGA−JRA (15°S-15°N, 110°E-180°)
LN_CP	TOGA−JRA (15°S-15°N, 180°-110°W)

LIST OF FIGURES

Fig. S1. Stationary wave components of the 1000 hPa (left) and 300 hPa (right) stream function anomalies simulated by (a) (d) "TOGA_H+JRA_T+JRA_B", (b) (e) "JRA_H+TOGA_T+JRA_B", (c) (f) "JRA_H+JRA_T+TOGA_B" experiments in Table 1. 4

Fig. S2. Stationary wave components of the 300 hPa stream function anomalies simulated by (a) "TOGA_H+TOGA_T+JRA_B" experiment, and (b) the difference between "TOGA_H+TOGA_T+JRA_B" and "JRA_all" experiments. 5

Fig. S3. Stationary wave components of the 1000 hPa (left) and 300 hPa (right) stream function anomalies simulated by (a) (d) "JRA_trop", (b) (e) "TOGA_trop" experiments in Table 2; (c) (f) their difference. 6

Fig. S4. Stationary wave components of the 1000 hPa (left) and 300 hPa (right) stream function anomalies simulated by (a) (d) "JRA_xtrop", (b) (e) "TOGA_xtrop" experiments in Table 2; (c) (f) their difference. 7

Fig. S5. Tropical diabatic heating during El Niño events for (a) JRA55's DJ average, (b) JRA55's FM average, (c) CESM1 TOGA simulations' DJ average, (d) CESM1 TOGA simulation's FM average. The top panels are for the vertical cross section averaged over 15°S-15°N. The bottom panels are for the horizontal distribution at 500 hPa. 8

Fig. S6. Tropical diabatic heating bias in CESM1 TOGA simulations when compared to (a) JRA55, (b) NCEP-NCAR (R1), (c) ERA20C, (d) ERAI, (e) ERA5, and (f) CFSR datasets during FM of the El Niño events in 1980–2009. 9

Fig. S7. Similar to Fig.6 but by imposing the CP diabatic heating biases (a)-(b) north (0°-15°N, 180°-110°W) and (c)-(d) south (15°S-0°, 180°-110°W) of the equator separately. 10

Fig. S8. Evolution of the tropical diabatic heating bias by applying the iterative bias-correction technique. 11

Fig. S9. Stationary wave components of the 300 hPa stream function anomalies simulated by the SW model for understanding the residual North Pacific cyclonic circulation bias seen in "*iter* 9" (Fig. 11). Only the diabatic heating bias over the CP in "*iter* 9" (Fig. 9(j)) is used to force the SW model. 12

Fig. S10. Extratropical diabatic heating bias in (a) NINO and (b) "*iter* 9" experiment. the area that exceeds 95% confidence level is stippled. 13

Fig. S11. (a) DJ and (b) FM-averaged tropical diabatic heating bias in CESM1 TOGA simulations during La Niña events from 1958 to 2010. The top panels are for the vertical cross section averaged over 15°S-15°N. The bottom panels are for the horizontal distribution at 500 hPa. The area that exceeds 95% confidence level is stippled. 14

Fig. S12. Stationary wave components of the 300 hPa stream function anomalies simulated by (a) "LN_trop", (b) "LN_IO", (c) "LN_WP", and (d) "LN_CP" experiments in Table S1. 15

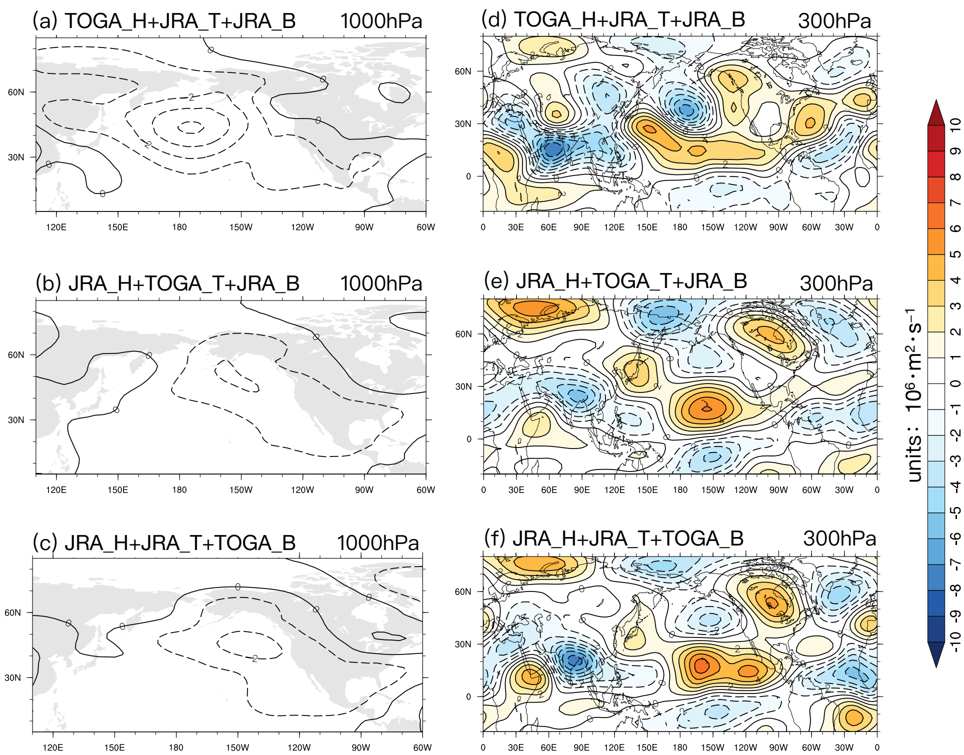

Fig. S1. Stationary wave components of the 1000 hPa (left) and 300 hPa (right) stream function anomalies simulated by (a) (d) “TOGA_H+JRA_T+JRA_B”, (b) (e) “JRA_H+TOGA_T+JRA_B”, (c) (f) “JRA_H+JRA_T+TOGA_B” experiments in Table 1.

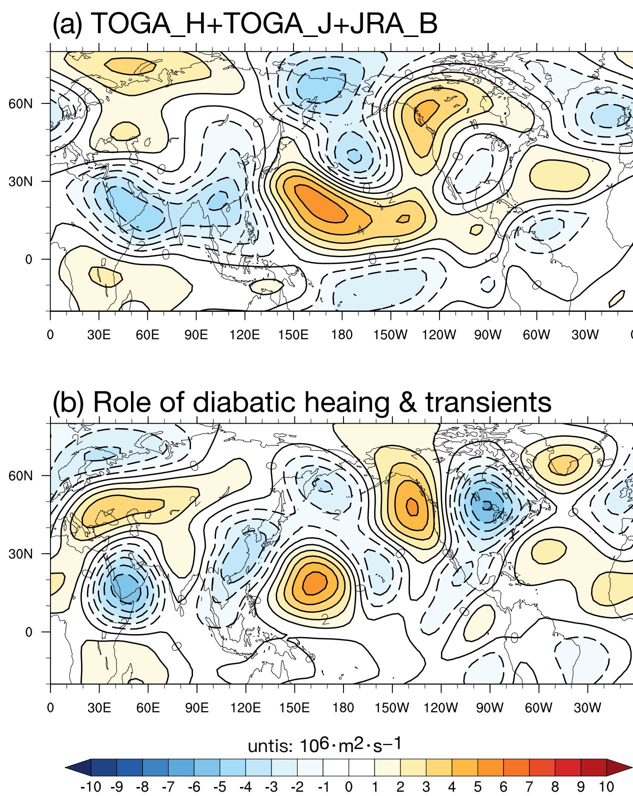

52 Fig. S2. Stationary wave components of the 300 hPa stream function anomalies simulated by (a) "TOGA_H+TOGA_T+JRA_B" experiment, and (b) the difference between "TOGA_H+TOGA_T+JRA_B" and "JRA_all" experiments.

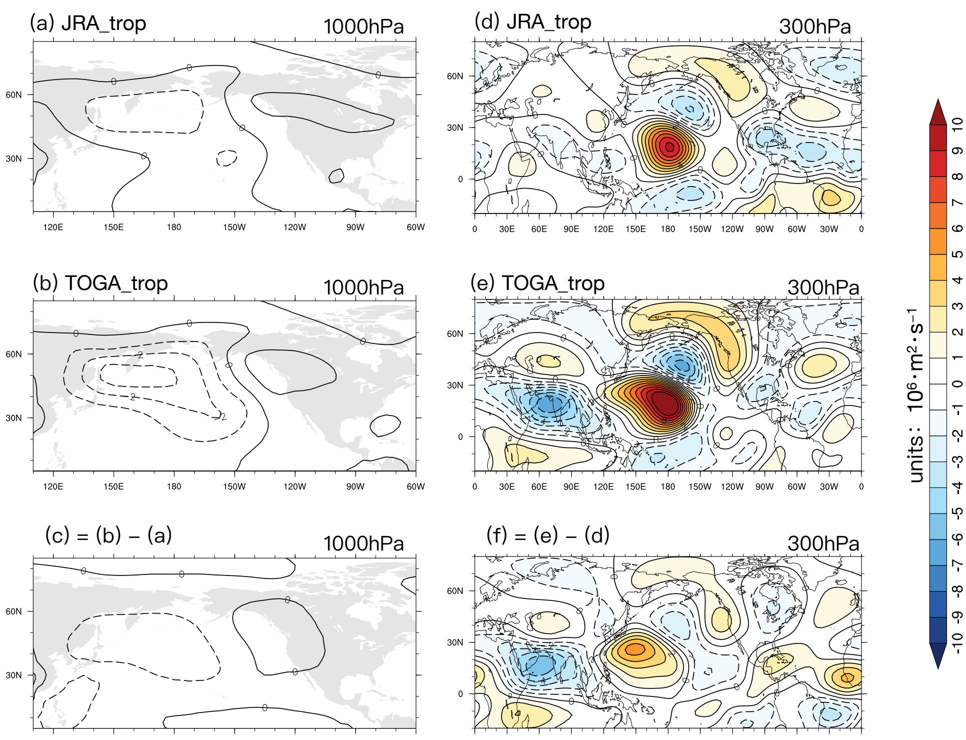

Fig. S3. Stationary wave components of the 1000 hPa (left) and 300 hPa (right) stream function anomalies simulated by (a) (d) "JRA_trop", (b) (e) "TOGA_trop" experiments in Table 2; (c) (f) their difference.

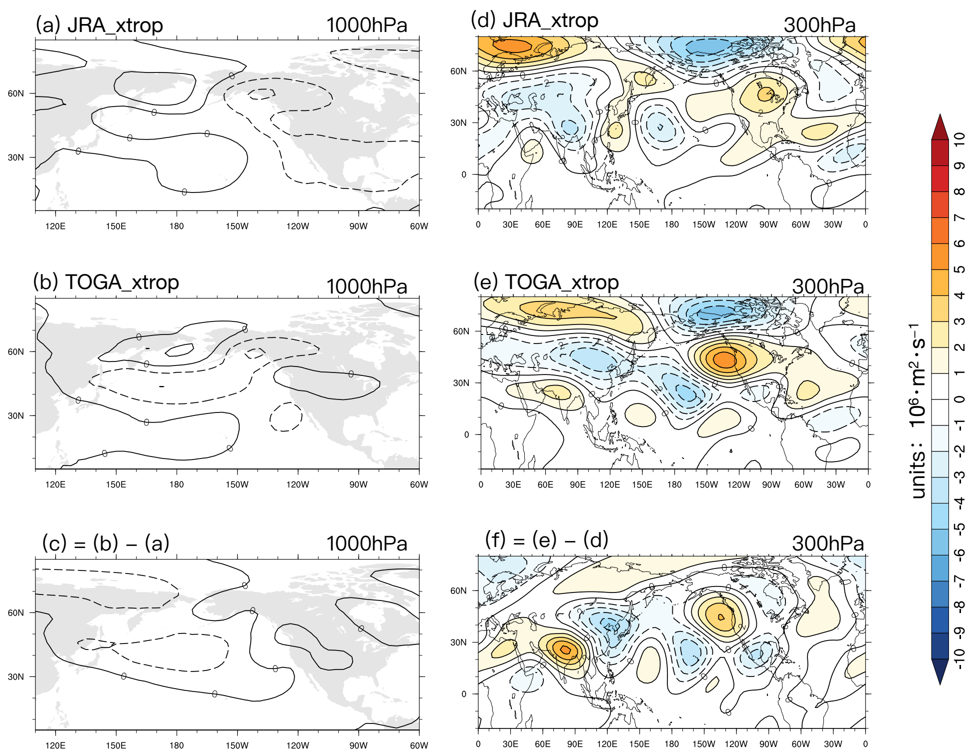

Fig. S4. Stationary wave components of the 1000 hPa (left) and 300 hPa (right) stream function anomalies simulated by (a) (d) "JRA_xtrop", (b) (e) "TOGA_xtrop" experiments in Table 2; (c) (f) their difference.

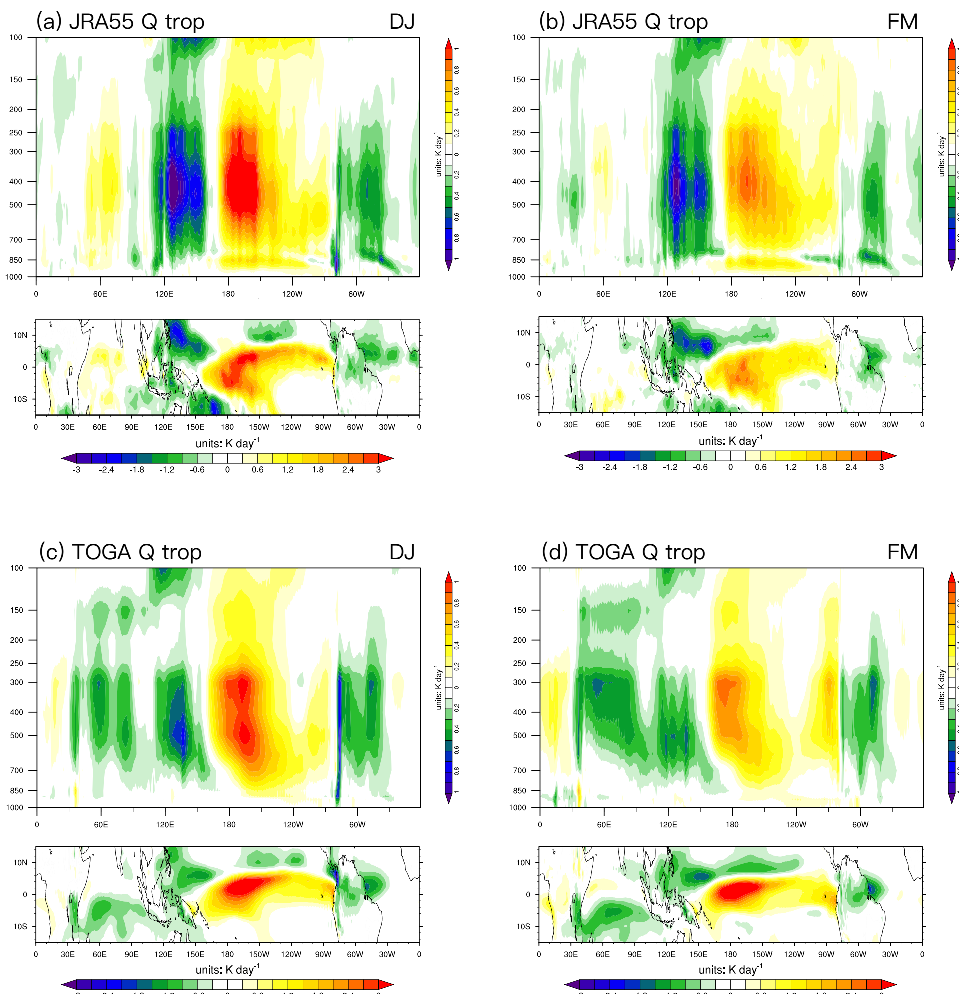

Fig. S5. Tropical diabatic heating during El Niño events for (a) JRA55's DJ average, (b) JRA55's FM average, (c) CESM1 TOGA simulations' DJ average, (d) CESM1 TOGA simulation's FM average. The top panels are for the vertical cross section averaged over 15°S-15°N. The bottom panels are for the horizontal distribution at 500 hPa.

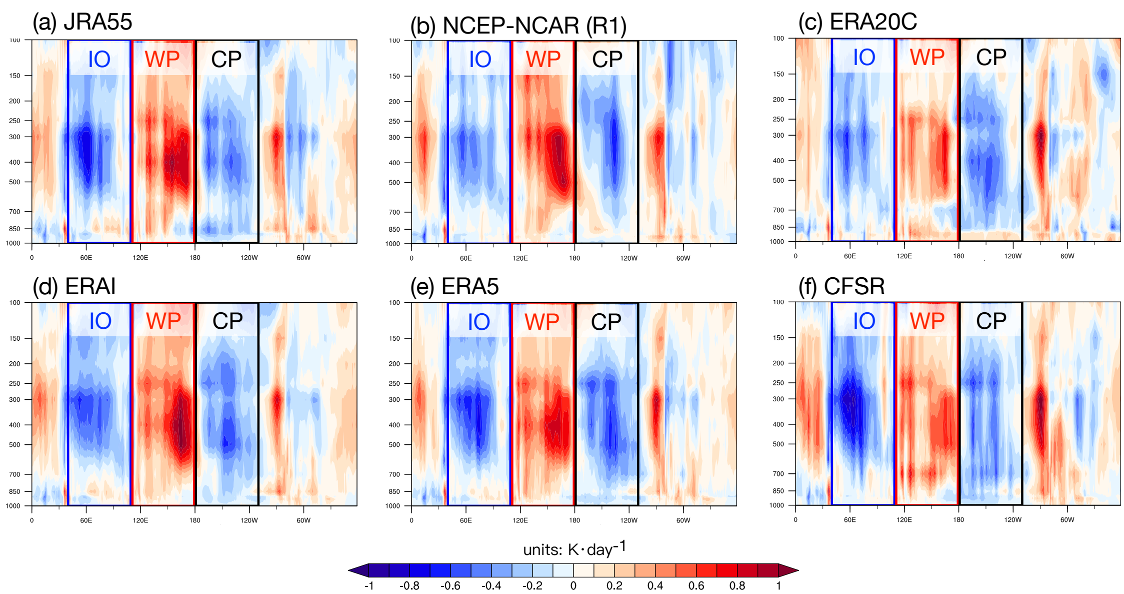

63 Fig. S6. Tropical diabatic heating bias in CESM1 TOGA simulations when compared to (a) JRA55, (b)
64 NCEP-NCAR (R1), (c) ERA20C, (d) ERAI, (e) ERA5, and (f) CFSR datasets during FM of the El Niño events
65 in 1980–2009.

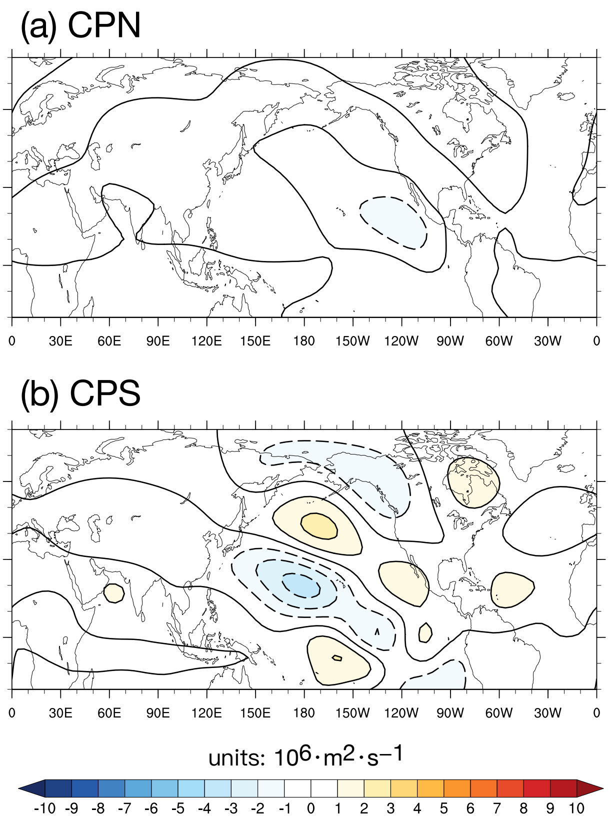

Fig. S7. Similar to Fig.6 but by imposing the CP diabatic heating biases (a)-(b) north (0°-15°N, 180°-110°W) and (c)-(d) south (15°S-0°, 180°-110°W) of the equator separately.

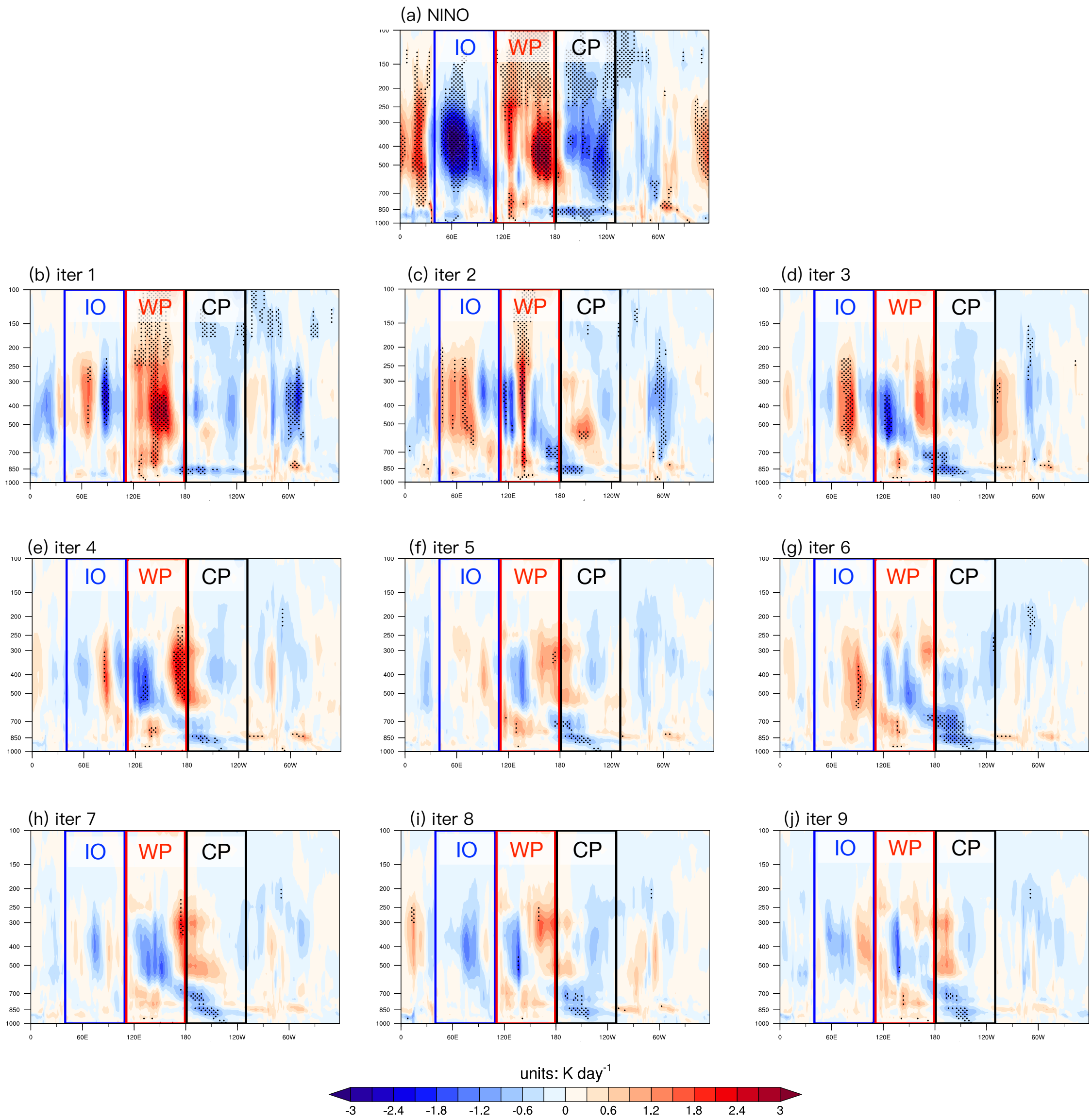

Fig. S8. Evolution of the tropical diabatic heating bias by applying the iterative bias-correction technique.

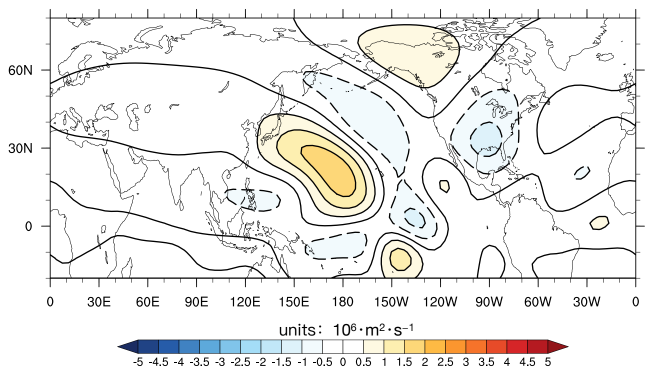

Fig. S9. Stationary wave components of the 300 hPa stream function anomalies simulated by the SW model for understanding the residual North Pacific cyclonic circulation bias seen in "*iter* 9" (Fig. 11). Only the diabatic heating bias over the CP in "*iter* 9" (Fig. 9(j)) is used to force the SW model.

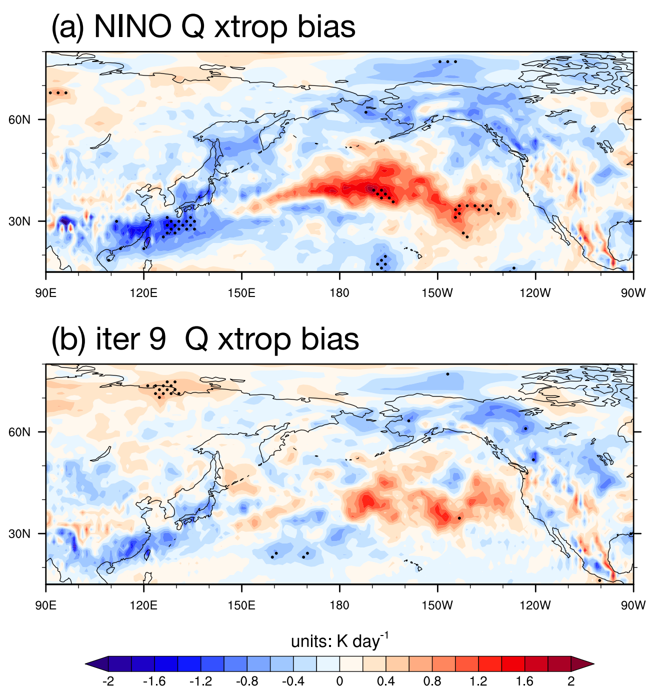

Fig. S10. Extratropical diabatic heating bias in (a) NINO and (b) "*iter* 9" experiment. the area that exceeds 95% confidence level is stippled.

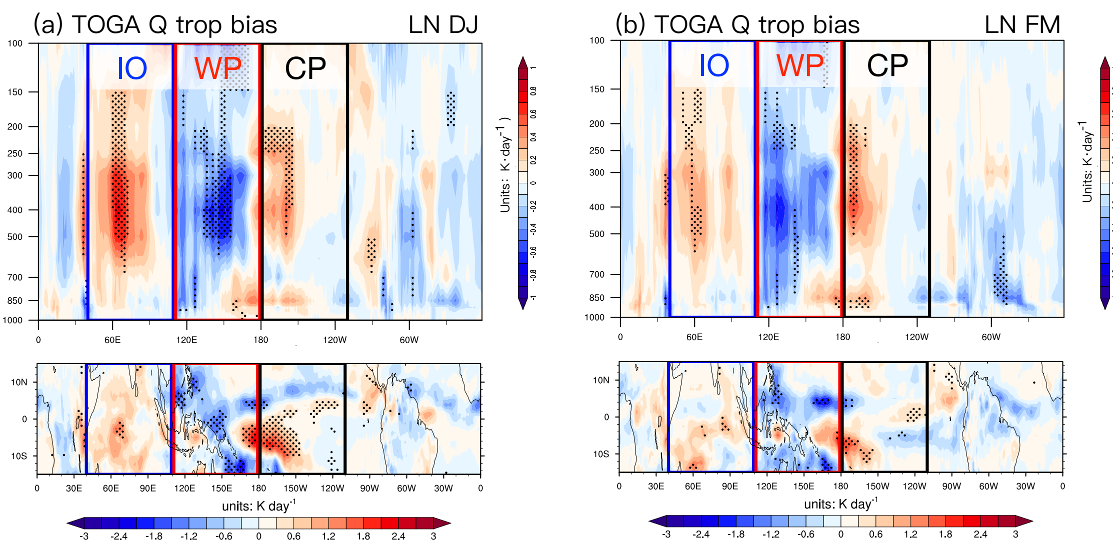

Fig. S11. (a) DJ and (b) FM-averaged tropical diabatic heating bias in CESM1 TOGA simulations during La Niña events from 1958 to 2010. The top panels are for the vertical cross section averaged over 15°S-15°N. The bottom panels are for the horizontal distribution at 500 hPa. The area that exceeds 95% confidence level is stippled.

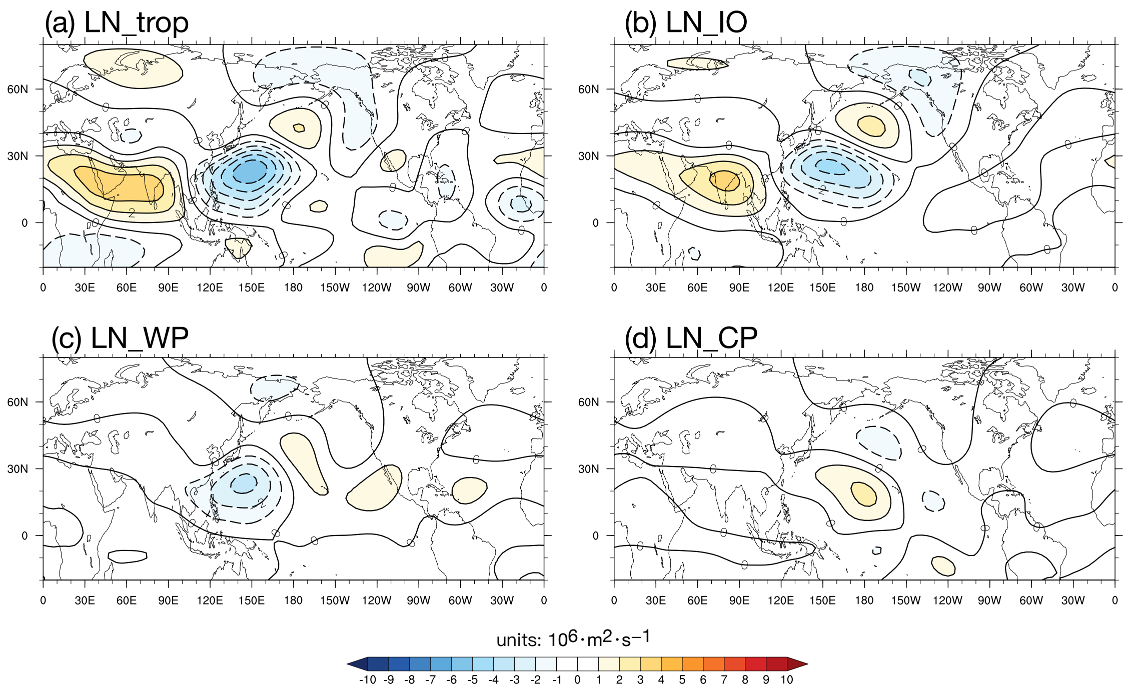

77 Fig. S12. Stationary wave components of the 300 hPa stream function anomalies simulated by (a) "LN_trop",
78 (b) "LN_IO", (c) "LN_WP", and (d) "LN_CP" experiments in Table S1.